

# Automatic multigrid mesh refinement strategy for precise localized stress concentration simulation

H. LIU<sup>a,b</sup>, I. RAMIÈRE<sup>a</sup>, F. LEBON<sup>b</sup>

a. DEN/DEC/SESC/LSC, CEA Cadarache, F-13108 Saint-Paul Lez Durance, France

b. Laboratoire de Mécanique et d'Acoustique, CNRS, UPR 7051, Aix-Marseille Univ, Centrale Marseille, 31, Chemin Joseph Aiguier, F-13402 Marseille Cedex 20, France

## Résumé :

*L'interaction mécanique pastille-gaine est un phénomène se produisant dans les réacteurs à eau pressurisée et pouvant mettre à défaut l'intégrité de la gaine entourant le combustible. Dans cet article, la méthode multigrille Local Defect Correction (LDC) est utilisée afin d'améliorer la précision de la simulation de ce phénomène. A partir d'un maillage initial, cette méthode consiste à ajouter récursivement des sous-grilles locales dans des zones où une solution précise est recherchée. Afin de détecter automatiquement les zones à raffiner, la méthode LDC est couplée avec l'estimateur d'erreur a posteriori de type Zienkiewicz et Zhu. Cet estimateur se base sur le fait que les contraintes obtenues par la méthode des éléments finis sont discontinues entre éléments. Il permet ainsi de détecter les zones de singularité de contraintes. La stratégie proposée permet de raffiner automatiquement le maillage dans les zones de concentration de contraintes et également d'arrêter le raffinement quand la solution est suffisamment précise ou lorsque le raffinement n'apporte plus d'amélioration de la solution. Les résultats numériques obtenus sur des cas tests 2D élastiques avec discontinuité de chargement montrent l'efficacité de cette stratégie mais également les limites de l'estimateur d'erreur a posteriori de type Zienkiewicz et Zhu.*

## Abstract :

*The Pellet-Cladding mechanical Interaction (PCI) occurs in Pressurized Water Reactors and might pose a risk to the integrity of the cladding containing the fuel. In this paper, the Local Defect Correction multigrid method (LDC) is performed in order to improve the PCI simulation accuracy. From an initial coarse mesh, this method consists in recursively adding local sub-grids in zones where higher accuracy is required. In order to automatically detect the zones to be refined, the LDC method is coupled with the Zienkiewicz-Zhu a posteriori error estimator. This estimator is based on the stress discontinuities between elements obtained by the finite element method. It provides hence a tool to detect the stress singularity zones. The strategy proposed enables us to automatically refine the mesh around the stress concentration zones and to stop the refinement process when the solution is accurate enough or when the refinement does not improve the solution accuracy anymore. The numerical results on 2D elasticity test cases show the efficiency of this strategy but also the limit of the Zienkiewicz-Zhu a posteriori error estimator.*

**Mots clefs :** Automatic mesh refinement, Local Defect Correction method, Zienkiewicz and Zhu a posteriori error estimator, Stress concentration localization

# 1 Introduction

In Pressurized Water Reactors, the Pellet-Cladding mechanical Interaction (PCI) happens in early stage of irradiation. Precise numerical simulations of this localized phenomenon require cells of  $1 \mu m$  for a structure of  $1 cm$ . Actual personal computers are not able to reach this accuracy in reasonable computational time and memory space. In order to overcome these difficulties, it is proposed here to use the Local Defect Correction (LDC) multigrid method introduced by Hackbush [1]. This method consists in recursively adding local sub-grids in zones where higher accuracy is required. In order to automatically detect the zones to be refined, a coupling between the LDC multigrid method and the Zienkiewicz-Zhu (ZZ) *a posteriori* error estimator [2] is proposed. A strategy for coupling the LDC multigrid method with the ZZ estimator was already introduced in [3, 4]. However, strategy introduces an arbitrary coefficient which may depend on the problem under consideration and on the user knowledge. Another strategy, proposed in [5] and recalled in this paper, has been developed in order to avoid this dependence. The numerical results presented in [5] on 2D axisymmetric test cases show that this method works well. The numerical results for the 2D plane strain test case presented in this paper confirm the efficiency of this automatic strategy but also show the limit of this method due to the ZZ error estimator.

This paper is organized as follows. The section 2 focuses on the coupling of the LDC method with the ZZ *a posteriori* error estimator. The section 3 introduces briefly the PCI phenomenon and the associated simplified 2D plane strain test case. Finally, numerical results that demonstrate the automatic detection and refinement of stress concentration zones are presented in section 4.

## 2 Automatic mesh refinement strategy

### 2.1 The LDC method

The Local Defect Correction method (LDC) [1] method is an Adaptive Mesh Refinement method based on a local multigrid process [6, 7]. This methods starts with a global coarse grid defined on the whole domain. Then local sub-grids with finer and finer mesh steps are recursively added in zones of interest, see Figure 1. Prolongation and restriction operators are used to link the different levels of grids. The problems arising on all the grids are solved sequentially until the solution of the coarsest grid has converged. This iterative process can be described by a  $\wedge$ -cycle, see Figure 2. In the following, the two-grids LDC method is briefly presented. The reader can refer to [1, 3] for more details.

A problem ( $\mathcal{P}$ ) well-defined on an open-bounded domain  $\Omega$  with boundary  $\partial\Omega$  is considered. This problem is discretized on a coarse grid  $G_H$  of boundary  $\Gamma_H$  with grid size  $H$ . The discretized problem is denoted ( $\mathcal{P}_H$ ). We define a local subdomain  $\Omega_1 \subset \Omega$  covering the zone of interest of  $\Omega$ .  $\Omega_1$  is discretized with a local grid  $G_h$  of boundary  $\Gamma_h$  with grid size  $h < H$ . The discretization of ( $\mathcal{P}$ ) on  $G_h$  is denoted ( $\mathcal{P}_h$ ).

The LDC algorithm then writes :

- Initialization : Solve the discretized problem ( $\mathcal{P}_H$ ) on  $G_H$ .
- Until the solution of ( $\mathcal{P}_H$ ) converges between two iteration cycles do :
  - Prolongation step : Define the boundary conditions of the local problem ( $\mathcal{P}_h$ ). On the boundary part  $\Gamma_h \cap \partial\Omega$ , original problem ( $\mathcal{P}$ ) boundary conditions are imposed. On  $\Gamma_h \setminus \partial\Omega$ , Dirichlet boundary conditions are obtained by projecting the coarse problem ( $\mathcal{P}_H$ ) solution, see Figure 3.

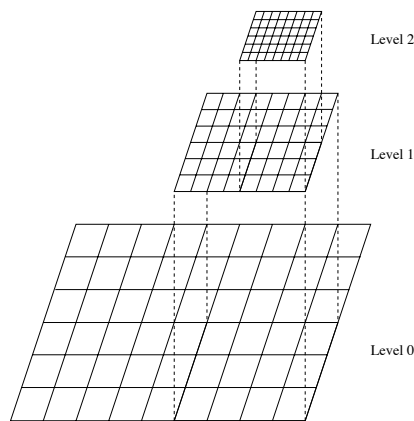


FIGURE 1 – Example of hierarchical meshes used in LDC method

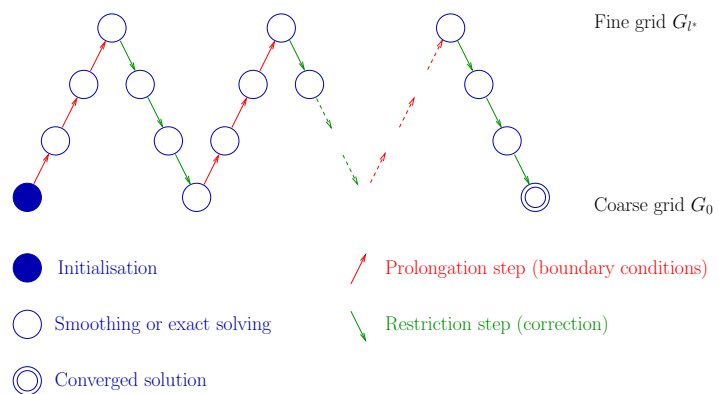


FIGURE 2 – Representation of the iterative process in  $\Lambda$ -cycle

- Solve the local discretized problem ( $\mathcal{P}_h$ ).
- Restriction step : Calculate the defect in order to correct the coarse problem ( $\mathcal{P}_H$ ). The fine problem ( $\mathcal{P}_h$ ) solution is restricted on the set  $A_H$  of coarse nodes of  $G_H$  strictly included in  $G_h$ . The defect of the problem ( $\mathcal{P}_H$ ) is then evaluated on the interior nodes of  $A_H \cup \Gamma_H$  in the sense of the discretization scheme, see Figure 4.
- ( $\mathcal{P}_H$ ) is then solved by adding the defect to the initial source term.

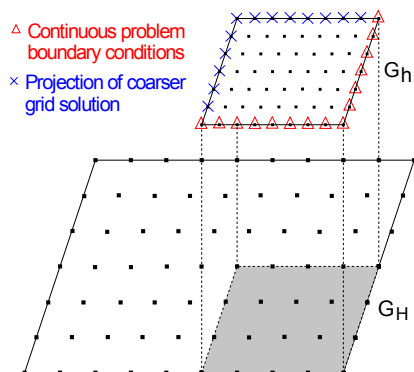


FIGURE 3 – Example of boundary conditions on  $G_h$  for hierarchical meshes

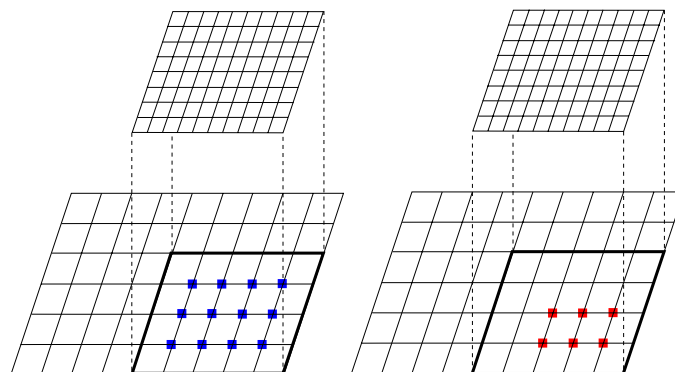


FIGURE 4 – Example of restriction zone  $A_H$  (on the left) and correction zone (on the right) in the case of a 5-point stencil operator for hierarchical meshes

The multigrid algorithm is obtained by recursively applying the two-grids algorithm [1, 3]. This method has the main advantage to consider the solvers as "black-box". It should also be noted that it is a generic method : solver, refinement ratio, mesh type, model, etc, could be different (or not) between the different levels of refinement. However, with the definition of the correction zone, this method requires a sufficiently large refinement zone to be efficient [1].

## 2.2 Zienkiewicz and Zhu *a posteriori* error estimators

*A posteriori* error estimators [8, 9, 2] provide a technique to automatically detect the elements with higher error from a preliminary calculation.

Based on the fact that the stress field of the Lagrange finite element method is discontinuous between elements, recovery-based error estimators proposed by Zienkiewicz and Zhu [2, 10] intend to construct

a smoothed stress field. These estimators propose to recover the nodal values of stresses by using a minimization method and then construct a continuous stress field using displacement shape functions. The error estimator is evaluated by the difference between the finite element stress solution and the smoothed stress field. Because of its efficiency, the good results it provides and the easiness of its implementation, these estimators are widely used in industrial codes such as Cast3M or Code\_Aster.

### 2.3 Coupling the LDC with the ZZ estimators

In order to automatically detect the zones of interest, we couple the ZZ estimator within the LDC method. The coupling between the ZZ estimator and the LDC method can be easily realized as both approaches are sequentially applied : at the first prolongation step, after each calculation, the ZZ estimator is applied on each level to detect the zones of interest. These sub-grids are then used in the sequel of the LDC process.

In order to automatically detect the zones of interest with the error indicator estimated by ZZ estimator, Barbie et al [3, 4] have proposed to refine the elements  $K$  for which the indicator is superior to  $\alpha$  of the maximum error :

$$e_K > \alpha(\max_{L \subset G_l} e_L) \quad (1)$$

with

$$0 \leq \alpha \leq 1, \alpha \text{ a unknown coefficient}$$

This strategy is easy to implement but requires the knowledge of the factor  $\alpha$  which may depend on the considered problem. Moreover, an arbitrary stopping criteria has to be defined because this indicator never stops.

The following automatic refinement procedure is proposed (see also [5]) to overcome these disadvantages.

The error between the finite element solution and the smoothed stress fields used by the Zienkiewicz and Zhu *a posteriori* error estimators calculated in energy norm writes :

$$\|e_K\|_E = \left( \frac{\int_K (\sigma^* - \sigma_h) : (\varepsilon^* - \varepsilon_h) dK}{\int_K \sigma^* : \varepsilon^* dK} \right)^{1/2} \quad (2)$$

with  $\sigma^*$  smoothed stress solution,  $\sigma_h$  the finite element stress solution,  $C$  is the stiffness tensor and  $\varepsilon^* = [C]^{-1}\sigma^*$ ,  $\varepsilon_h = [C]^{-1}\sigma_h$ .

The automatic procedure of refinement proposed in [5] works directly on the elements for which the stress error is superior to a relative threshold  $\beta$  :

$$\|e_K\|_E > \beta \quad (3)$$

When the refinement stops, the estimated global error  $\|e_\Omega\|_E$  is guaranteed to be inferior to the relative threshold  $\beta$ .

When the problem presents a singularity, the error between the finite elements solution and the smoothed solution could be always superior to the relative threshold. So an additional stopping criteria for the automatic generation of the sub-grids has to be defined : when the measure of the detected zone is

inferior to the measure of one coarsest element, the generation of sub-grids is stopped. In fact, following the LDC algorithm (see section 2.1), the local zone detected in this case is too small to correct the coarsest solution.

### 3 The PCI phenomenon and the associated simplified test case

#### 3.1 The PCI phenomenon

The PCI phenomenon occurs during the irradiation in Pressurized Water Reactors. The fuel pellets crack at the early stages of irradiation. Meanwhile, the pressure of the water in the primary circuit leads to the cladding's creep and the pellets swell due to the accumulation of gaseous fission products within the material. The initial gap between the pellets and the cladding decreases and discontinuous contacts appear. At the same time, the fragmented pellets deform in a hourglass shape due to high temperature gradient. All these phenomena induce localized high stress concentrations on the cladding in front of the inter-pellet plane that might lead to fuel rod failure under certain circumstances.

#### 3.2 The simplified 2D( $r,\theta$ ) test case

A test case with the plane strain hypothesis, called the 2D( $r,\theta$ ) test case, is introduced. This test case is designed to simulate the effect of the pellet cracking on the cladding. Only the cladding is considered here and the contact with the pellet is represented by a pressure discontinuity (due to the cracks) on the internal radius of the cladding. We focus on the elastic response of the cladding with the Young's modulus  $E = 100 \text{ GPa}$  and the Poisson's ratio  $\nu = 0.3$ . As the pellet is assumed to crack in a regular way (see figure 5a), only 1/16 of the cladding is modelled. The definition of the problem is represented on Figure 5b.

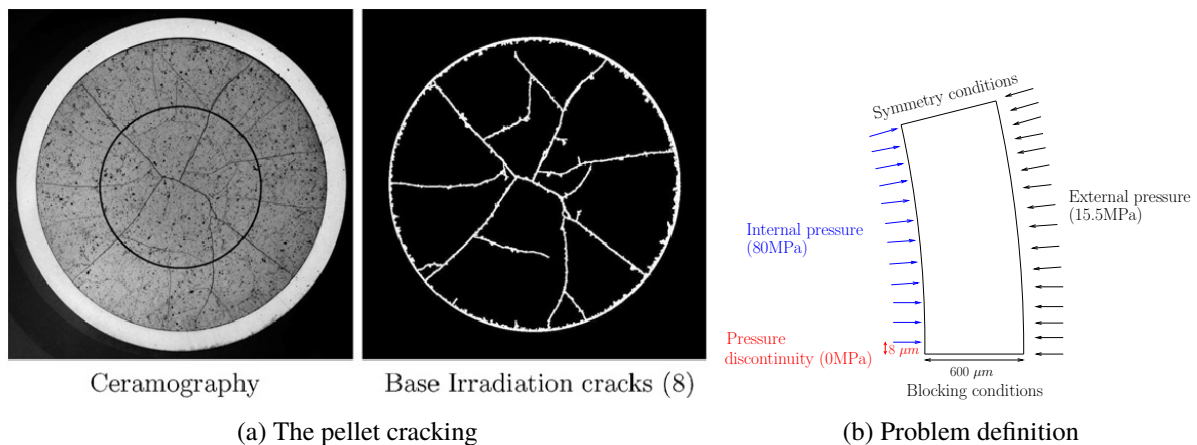


FIGURE 5 – 2D ( $r,\theta$ ) test case

A reference solution obtained with a very fine mesh (quasi-uniform mesh of  $2\mu\text{m}$  mesh step) is used to validate the proposed strategy.

### 4 Numerical results

We apply the strategy of coupling LDC method with ZZ estimator introduced in the section 2.3 to the 2D( $r,\theta$ ) test case. Figure 6 presents the generated sub-grids for an initial mesh size equal to  $54.5 \mu\text{m}$  and

a threshold  $\beta$  of 1%. As expected, the local sub-grids are located around the pressure discontinuity zone where the stresses present a singularity.

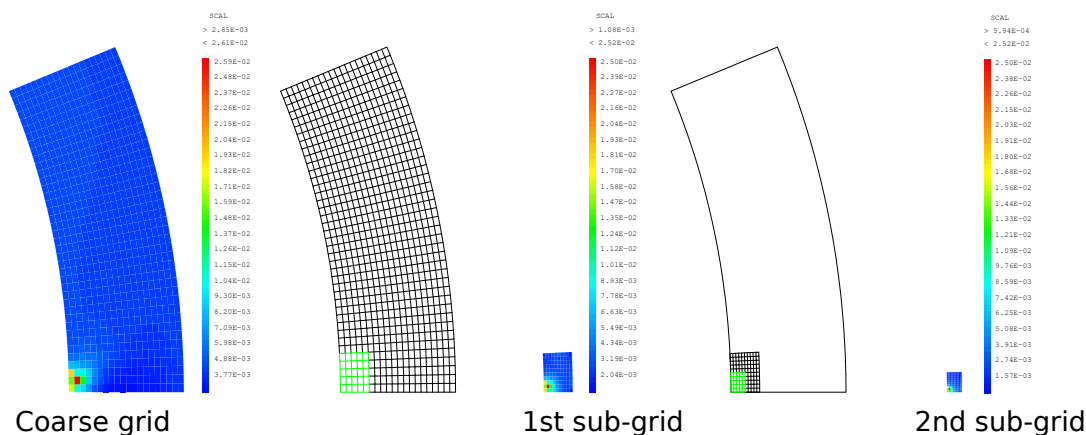


FIGURE 6 – Exemple for the 2D( $r,\theta$ ) test case · Coarse mesh size :  $54.5 \mu\text{m}$  ·  $\beta = 1\%$

This example shows that the proposed coupling strategy works very well in automatically detecting the zones to be refined.

Then the LDC algorithm is applied on these sub-grids. The iterative process is considered as convergent when the  $L_2$  norm relative error between two successive coarse solutions  $u_0$  is smaller than  $1.10^{-5}$  :

$$\frac{\|u_0^k - u_0^{k-1}\|_{L_2}}{\|u_0^k\|_{L_2}} \leq 1.10^{-5} \quad (4)$$

The LDC method converges very fast. Typically, less than four iterations are required for convergence.

The coupling strategy has been tested on different coarse meshes and different thresholds. The results are reported in Table 1. The results of each calculation are presented in three lines : the first line indicates the number of sub-grid automatically generated, the second line contains the numbers of nodes of each sub-grid while the third line gives the relative error in energy norm between the convergent LDC composite solution and the reference solution.

Initial mesh		threshold			
		5%	2%	1%	0.50%
hi	sub-grid number :	0	1	2	3
	number of nodes :	231	231/81	231/861/121	231/861/289/195
	relative error :	7.05%	3.26 %	1.27%	0.476%
hi/2	sub-grid number :	0	1	2	3
	number of nodes :	861	861/81	861/121/121	861/289/195/195
	relative error :	3.19 %	1.27%	0.462%	0.457%
hi/4	sub-grid number :	0	1	2	3
	number of nodes :	3321	3321/81	3321/121/121	3321/195/195/285
	relative error :	1.22%	0.294%	0.289%	0.287%

TABLE 1 – LDC-ZZ coupling strategy on the 2D ( $r,\theta$ ) test case with mesh step hi =  $109 \mu\text{m}$

The first conclusion to be drawn from Table 1 is that the generation of sub-grids automatically stops. Table 1 also shows the efficiency of the LDC method. The errors are quickly reduced by adding local grids with a limited number of degrees of freedom. So it is more interesting to begin with a coarse

enough grid then add local sub-grids rather than begin with a too fine mesh. Moreover, at the end of the calculation, the errors obtained are generally lower than the thresholds. Concerning the ZZ error estimator, it seems that for coarse meshes (see row 1 of Table 1) the estimator underestimates the finite element error while for fine meshes this estimator overestimates the finite element error (see row 3 of Table 1 where more sub-grids are generated with the decrease of the threshold whereas it was not necessary).

However, only the results for the initial coarsest mesh (with mesh size equal to  $109 \mu\text{m}$ ) are not as good as expected with the three largest thresholds (5%, 2%, 1%). To find out the reason of this behaviour, the relative error estimated by the ZZ estimator and the relative stress error between the finite element solution and the reference solution are compared on Figure 7.

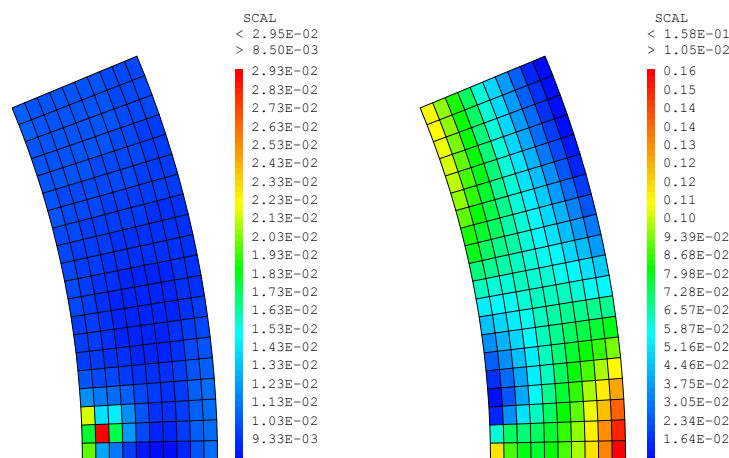


FIGURE 7 – Error estimated by the ZZ estimator (at left) and error between the finite element solution and the reference solution (at right) (mesh size :  $109 \mu\text{m}$ )

For this coarsest mesh, the major error between the finite element solution and the reference solution is located around the bottom right corner of the mesh. This is due to a bad approximation of the boundary condition. This kind of error could not be detected by the ZZ estimator which focuses only on the smoothness of the solution. In these zones, the ZZ estimator underestimates the finite element error. This figure can also explain why the result for the same initial mesh size with a threshold  $\beta$  of 0.5% is much better. Indeed, in this case, the strategy leads to refine all the domain and hence the boundary condition is better approximated.

## 5 Conclusion

In order to accurately simulate the stress concentration zone of the PCI, a strategy to couple the Local Defect Correction method with the Zienkiewicz and Zhu *a posteriori* error estimator in an user-independent way has been proposed. This strategy works well for the test cases whose errors are mainly caused by a stress singularity. The LDC method appears to be a powerful adaptive mesh refinement tool. The ZZ error estimator well detects stress singularity zones but is unable to detect the zones where the smooth solution is not accurate enough. For these situations, it could be interesting to combine another error estimator with the LDC method in order to more accurately detect all the zone to be refined.

## Références

- [1] W. Hackbusch, “Local Defect Correction Method and Domain Decomposition Techniques,” *Computing Suppl. Springer-Verlag*, vol. 5, pp. 89–113, 1984.
- [2] O. Zienkiewicz and J. Zhu, “A simple error estimator and adaptive procedure for practical engineering analysis,” *International Journal for Numerical Methods in Engineering*, vol. 24, pp. 337–357, 1987.
- [3] L. Barbié, I. Ramière, and F. Lebon, “Strategies around the local defect correction multi-level refinement method for three-dimensional linear elastic problems,” *Computers and Structures*, vol. 130, pp. 73–90, 2014.
- [4] L. Barbié, I. Ramière, and F. Lebon, “An automatic multilevel refinement technique based on nested local meshes for nonlinear mechanics,” *Computers & Structures*, vol. 147, pp. 14–25, 2015.
- [5] H. Liu, I. Ramière, and F. Lebon, “Local defect correction method coupled with the zienkiewicz-zhu a posteriori error estimator in elastostatics solid mechanics,” in *17th Copper mountain Conference on Multigrid Methods*, 2015. 22-27 March 2015, Copper Mountain, U.S.A.
- [6] P. Angot, J. Caltagirone, and K. Khadra, “Une méthode adaptative de raffinement local : la Correction de Flux à l’Interface,” *Comptes Rendus de l’Académie des Sciences de Paris*, vol. 315, pp. 739–745, 1992.
- [7] A. Brandt, “Multi-level adaptive solutions to boundary-value problems,” *Mathematics of Computation*, vol. 31, pp. 333–390, 1977.
- [8] I. Babuška and W. Rheinboldt, “A-posteriori error estimates for the finite element method,” *International Journal for Numerical Methods in Engineering*, vol. 12, pp. 1597–1615, 1978.
- [9] P. Ladevèze and D. Leguillon, “Error estimate procedure in the finite-element method and applications,” *SIAM Journal on Numerical Analysis*, vol. 20, pp. 485–509, 1983.
- [10] O. Zienkiewicz and J. Zhu, “The superconvergent patch recovery and a posteriori error estimation. Part I : The recovery technique,” *International Journal for Numerical Methods in Engineering*, vol. 33, pp. 1331–1364, 1992.